Analytical and Bioanalytical Chemistry (2024) 416:1657–1665
https://doi.org/10.1007/s00216-024-05170-7

RESEARCH PAPER

Facile fabrication of Ti^{4+}-immobilized magnetic nanoparticles by phase-transitioned lysozyme nanofilms for enrichment of phosphopeptides

Jianru Li[1] · Nan Li[2] · Yawen Hou[1] · Miao Fan[1] · Yuxiu Zhang[1] · Qiqi Zhang[1] · Fuquan Dang[1]

Received: 28 November 2023 / Revised: 4 January 2024 / Accepted: 12 January 2024 / Published online: 6 February 2024

Abstract

In this study, titanium (IV)-immobilized magnetic nanoparticles (Ti^{4+}-PTL-MNPs) were firstly synthesized via a one-step aqueous self-assembly of lysozyme nanofilms for efficient phosphopeptide enrichment. Under physiological conditions, lysozymes readily self-organized into phase-transitioned lysozyme (PTL) nanofilms on Fe_3O_4@SiO_2 and Fe_3O_4@C MNP surfaces with abundant functional groups, including $–NH_2$, –COOH, –OH, and –SH, which can be used as multiple linkers to efficiently chelate Ti^{4+}. The obtained Ti^{4+}-PTL-MNPs possessed high sensitivity of 0.01 fmol μL^{-1} and remarkable selectivity even at a mass ratio of β-casein to BSA as low as 1:400 for phosphopeptide enrichment. Furthermore, the synthesized Ti^{4+}-PTL-MNPs can also selectively identify low-abundance phosphopeptides from extremely complicated human serum samples and their rapid separation, good reproducibility, and excellent recovery were also proven. This one-step self-assembly of PTL nanofilms facilitated the facile and efficient surface functionalization of various nanoparticles for proteomes/peptidomes.

Keywords Phase-transitioned lysozyme · Magnetic nanoparticles · Enrichment · Phosphopeptides

Introduction

As a ubiquitous post-translational modification, protein phosphorylation participates in multifarious biological processes, including metabolic pathways, epigenetic control, gene expression, and cell proliferation [1–4]. Mass spectrometry (MS) is critical for identifying phosphorylation sites and quantifying their dynamic changes in view of its high sensitivity, wide dynamic range, and fast analysis speed [5–9]. As we know, challenges always remained in phosphopeptides/proteins identification and characterization for the reason of low-abundance and the signal suppression from nonphosphopeptides/nonproteins in MS analysis [10–13]. Thus, selective phosphopeptide enrichment before MS analysis by a specific enrichment technique is an essential link for the in-depth study of the phosphoproteome [14, 15].

To date, numerous enrichment techniques, such as ion-exchange chromatography [16], metal oxide affinity chromatography [17–20], immune affinity capture, and immobilized metal ion affinity chromatography (IMAC) [21, 22], are commonly used to enrich phosphopeptides from non-phosphorylated peptides [23]. Among them, IMAC is a highly explored technique to enrich phosphopeptides, in which metal ions, such as Fe^{3+}, Cu^{2+}, Al^{3+}, Zn^{2+}, and Ti^{4+}, are chelated to adsorbents using specific bridging molecules, such as adenosine triphosphate [24, 25], glutathione [26], and polydopamine [27]. In most cases, monofunctional bridging molecules are covalently grafted to the surface of various adsorbents including polymer beads, porous materials, or nanoparticles via complicated synthesis chemistry, generally involving poisonous reagents and multistep treatments. Therefore, it is imperative to exploit a facile and rapid fabrication method for functionalizing adsorbents with abundant multiple functional ligands.

Jianru Li and Nan Li contributed equally to this work.

✉ Nan Li
linann@nwpu.edu.cn

✉ Fuquan Dang
dangfqn@snnu.edu.cn

[1] Key Laboratory of Analytical Chemistry for Life Science of Shaanxi Province, School of Chemistry and Chemical Engineering, Shaanxi Normal University, 620 West Chang′an Street, Xi'an 710119, China

[2] Frontiers Science Center for Flexible Electronics (FSCFE), Institute of Flexible Electronics (IFE) and Xi'an Institute of Biomedical Materials & Engineering (IBME), Northwestern Polytechnical University (NPU), Xi'an 710072, China

Lysozyme, denaturalized in tris(2-carboxyethyl)phosphine (TCEP) buffer under neutral pH conditions, readily self-organized into phase-transitioned lysozyme (PTL) nanofilms on various particle surfaces, exhibiting powerful interface combination to resist chemical and mechanical peeling under severe conditions [28, 29]. The abundant functional groups on the surface of PTL nanofilms, including $–NH_2$, –COOH, –OH, and –SH, may further immobilize metal ions by the synergistic chelation of multiple functional ligands. To verify this hypothesis, in this study, PTL nanofilms were first assembled on Fe_3O_4@SiO_2 and Fe_3O_4@C magnetic nanoparticles (MNPs) via the one-step aqueous self-assembly [28]. As expected, Ti^{4+}, which exhibited a strong affinity to the phosphate groups in phosphopeptides, were efficiently captured by PTL nanofilms to form the Ti^{4+}-PTL-MNPs by simple incubation in $Ti(SO_4)_2$ aqueous solution. The high sensitivity and selectivity for phosphopeptide enrichment from standard protein and human serum indicated great potential of the synthesized Ti^{4+}-PTL-MNPs for ultracomplex real samples analysis. Thus, the current method based on one-step aqueous self-assembly of PTL nanofilms provides a promising and environmentally friendly alternative to fabricating IMAC adsorbents for proteome/peptidome.

Experimental section

Materials and reagents

β-Casein (from bovine milk), bovine serum albumin (BSA), trypsin, urea, dithiothreitol (DTT), iodoacetamide (IAA), and 2,5-dihydroxybenzoic acid (DHB) were purchased from Sigma-Aldrich. Standard phosphopeptide (LRRApSLGGK) were purchased from Shanghai Apeptide Co., Ltd. Ammonium bicarbonate (NH_4HCO_3), and acetonitrile (ACN) were obtained from Merck (Darmstadt, Germany). Tetraethyl orthosilicate (TEOS), ferric chloride ($FeCl_3·6H_2O$), ethylene glycol (EG), trisodium citrate, sodium acetate (NaOAc), ethanol, 4-(2-hydroxyethyl)-1-piperazineethanesulfonic acid (HEPES), ammonium hydroxide ($NH_3·H_2O$, 25 wt %), lysozyme, tris (2-carboxyethyl) phosphine hydrochloride (TCEP), glucan, and glucose were obtained from Shanghai Chemical Reagents Company (Shanghai, China). All other reagents were of analytical grade from suppliers. The human serum sample was acquired from Shaanxi Normal University Hospital.

Characterization

Transmission electron microscopy (TEM) data was measured using a JEM-2100 microscope (JEOL, Japan). Fourier transform infrared (FT-IR) spectroscopy was performed using a Tensor 27 infrared spectrometer (Bruker, Billerica, MA). X-ray diffraction (XRD) measurements were conducted on X-ray powder diffractometer (Bruker D8 Advance). Environmental scanning electron microscopy (FEI Quanta 200) was used for energy-dispersive X-ray analysis (EDX) measurement. X-ray photoelectron spectroscopy (XPS) analyses were measured with an Axis Ultra XP spectrometer (Kratos Analytical Ltd., Manchester, UK). The saturation magnetization curves were obtained using vibrating-sample magnetometry (VSM) (Quantum Design, San Diego, USA).

Mass spectrometry analysis

All the mass spectrometry (MS) data was acquired using matrix-assisted laser desorption/ionization (MALDI)-time-of-flight (TOF) (MALDI-TOF) MS (Bruke Daltonics, Bremen, Germany) under the positive-ion reflector mode (laser wavelength: 337 nm). The other parameters including acceleration voltage (20 kV), grid voltage (65%), and delayed extraction time (180 ns) were used. Each MS was acquired as an average of 100 laser shots under the laser intensity of 50 Hz and mass range of 1,000–3,500. The database in version 201,412 of Uniprot rat reference proteome was used for MS data search.

Preparation of Fe_3O_4@SiO_2 and Fe_3O_4@C MNPs

The Fe_3O_4 particles were synthesized via a solvothermal reaction previously reported [1]. For the Fe_3O_4@SiO_2 MNPs synthesis [2], the above 100 mg Fe_3O_4 particles were added in dispersion of ethanol/ NH_3•H_2O/ H_2O (20/0.7/5, v/v/v) with ultrasonication for 40 min. Then 600 mL of TEOS was added dropwise into the mixture and stirring for 6 h for the growth of SiO_2 layer. Finally, the resulting Fe_3O_4@SiO_2 MNPs was collected by magnetic separation and washed 3 times before drying at 60 °C.

When preparing Fe_3O_4@C MNPs, glucose was used as carbon source according to the published work [3]. Briefly, 200 mg of Fe_3O_4 nanoparticles was suspended glucose solution (0.15 M) for ultrasonication. Then the mixture was transferred into Teflon-sealed autoclave for reaction of 6 h at 160 °C. Then the product of Fe_3O_4@C MNPs were rinsed with water for several times and finally dried at 60 °C overnight.

Recovery test of phosphopeptides enrichment

The quantitative approach of stable isotope dimethyl labeling was used to calculate the recovery of the Ti^{4+}-PTL-MNPs for phosphopeptides enrichment according to the previous reports [4]. Briefly, the heavy isotope-labeled phosphopeptide was enriched with Ti^{4+}-PTL-Fe_3O_4@SiO_2 and Ti^{4+}-PTL-Fe_3O_4@C, respectively. The above eluent was

mixed with the same amount of the light isotope-labeled phosphopeptide for MALDI-TOF MS analysis. The recovery of phosphopeptide was calculated according to the MS intensity ratio of heavy and light isotope-labeled phosphopeptide.

Synthesis of the Ti^{4+}-PTL-MNPs

The synthesized Fe_3O_4@SiO_2 [30, 31] and Fe_3O_4@C [32, 33] MNPs (10 mg) were homogeneously dispersed in 10 mL of mixed equal volume of lysozyme (3 mg ml^{-1} lysozyme in 9 mM HEPES buffer) and TCEP (45 mM TCEP in 9 mM HEPES buffer) buffer solutions, respectively, incubated at 37 °C for 30 min and washed alternately with ethanol and water to prepare PTL-coated MNPs [28]. Subsequently, the PTL-coated MNPs (10 mg) were incubated in 10 mL of a $Ti(SO_4)_2$ solution (100 mM) at 37 °C for 3 h to fix Ti^{4+} cations and collected by magnetic separation. Finally, the obtained Ti^{4+}-PTL-MNPs were washed with ethanol and water repeatedly, and dried overnight [34, 35].

Tryptic digestion of standard protein and human serum

Standard protein (β-casein or BSA) (6 mg) was added into 1.5 mL of a solution containing 8 M urea and 50 mM NH_4HCO_3 (pH 8.0) and incubated at 37 °C for 1.5 h. Protein mixture was then reduced and alkylated using DTT (10 µL, 500 mM) for 1 h under 60 °C and IAA (10 µL, 150 mM) for 30 min at room temperature (RT), respectively. Subsequently, the above solution was digested with trypsin at an enzyme/protein ratio of 1:40 (w/w) for 18 h at 37 °C and the reaction was stopped by adding 5 µL of formic acid (0.2%) to the solution. Finally, the tryptic digestion of protein solution was dialyzed for 48 h at room temperature (MWCO = 500 Da), lyophilized in a freeze dryer, stored at -20 °C, and diluted to the required concentration with different volume ratios of ACN/H_2O/HAC before use [23].

When preparing the real sample (human serum), 3.0 mL of human serum were gently mixed with 30 µL of NH_4HCO_3 (50 mM, pH 8.0) and then denatured at 100 °C for 5 min. After that, the mixture was digested by trypsin at an enzyme/protein ratio of 1:40 (w/w) at 37 °C for 18 h. Finally, 5 µL of formic acid (0.2%) was added to stop reaction, and then dialyzed and stored before use at -20 °C.

Phosphopeptide enrichment using tryptic standard protein and human serum digests

The Ti^{4+}-PTL-MNPs (1.5 mg) was added to 150 μL of a loading buffer (ACN/H_2O/HAC, 50/48/2, v/v/v) containing tryptic digests of β-casein or serum and vibrated for 3 min at RT to enrich phosphopeptides. After washing with 200 µL 50% ACN, 48% H_2O, and 2% HAC for three times, the Ti^{4+}-PTL-MNPs trapped with phosphopeptides were eluted with $NH_3 \cdot H_2O$ (100 µL, 0.5%) and was analyzed in MALDI-TOF MS measurement. The enrichment conditions including adsorption time and the loading buffer with different HAc concentrations of 5%, 3%, 2%, and 0.1% were optimized using β-casein digests [23].

Results and discussion

Characterization of synthesized Ti^{4+}-PTL-MNPs

PTL-coated Fe_3O_4@SiO_2 and Fe_3O_4@C MNPs were synthesized via the one-step aqueous self-assembly of lysozyme nanofilms in TCEP buffer at neutral pH as presented in Fig. 1. As demonstrated in published works [36, 37], the PTL nanofilms on the MNPs surface exhibited a series of multiple groups including -NH_2, -COOH, -OH, and -SH, which can be used as multiple linkers to efficiently chelate Ti^{4+} through coordination reactions, and then displayed a strong affinity with phosphate groups in phosphopeptides. Besides, the obtained Ti^{4+}-PTL-MNPs presented powerful interface combination to resist mechanical and chemical peeling under enrichment conditions, and may exhibit high mechanical stability from complex biological samples.

The microstructures and morphologies of the synthesized MNPs were investigated through TEM and SEM. The Fe_3O_4 MNPs had small nanocrystal clusters on the surfaces with diameters of ~ 150 nm (Fig. 2A). The Fe_3O_4@C and Fe_3O_4@SiO_2 MNPs showed relatively smooth surface with diameters of ~ 180 nm and ~ 200 nm, respectively, surrounded by light areas of silica and carbon shells, indicating a clear core–shell structure (Fig. 2B, C). However, no obvious changes in the morphology of PTL-coated Fe_3O_4@SiO_2 MNPs and Fe_3O_4@C MNPs (Fig. 2B, C, insets) were observed. The SEM images in Figs. 2D, E and F further proved the uniformity of the size and shape of the synthesized MNPs.

Next, the obtained Ti^{4+}-PTL-MNPs were further characterized by XPS, XRD, VSM, and EDX. In XPS spectra, Fe_3O_4 MNPs showed typical peaks of Fe and O which correlated well with previously reported results [31]. After coated with SiO_2 shells, the Si peaks was observed in the synthesized Fe_3O_4@SiO_2 MNPs while the Fe peaks almost disappeared (Fig. 3A, B). In the PTL-assembled MNPs, the N 1 s peak existed in the PTL amine groups was observed, and its contents was about 5% in the PTL-coated MNPs (Fig. S1, see Electronic Supplementary Material), confirming the PTL nanofilms successfully self-assembled on Fe_3O_4@SiO_2 and Fe_3O_4@C MNPs surface. EDX analysis clearly showed appearance of Ti element in the Ti^{4+}-PTL-MNPs, indicating successful loading of Ti^{4+} on the PTL-coated MNPs (Fig. S1, see Electronic

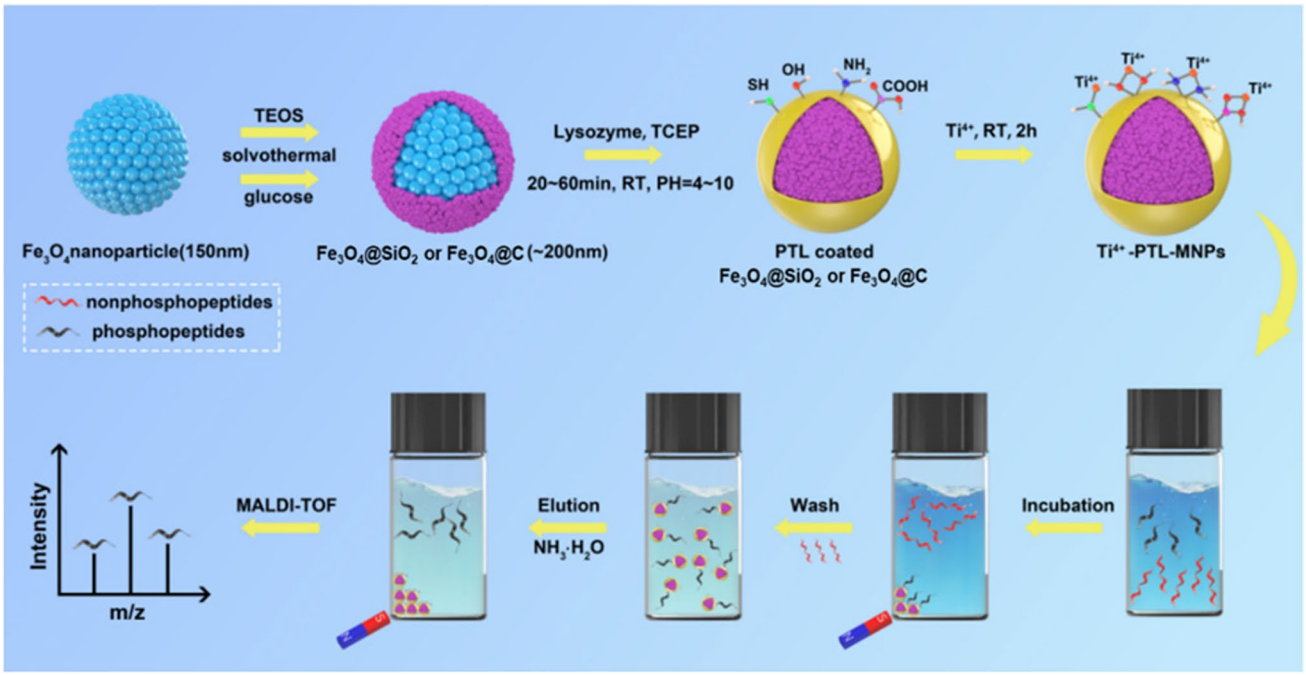

Fig. 1 Synthesis procedure of Ti^{4+}-PTL-MNPs and schematic diagram for phosphopeptides enrichment process

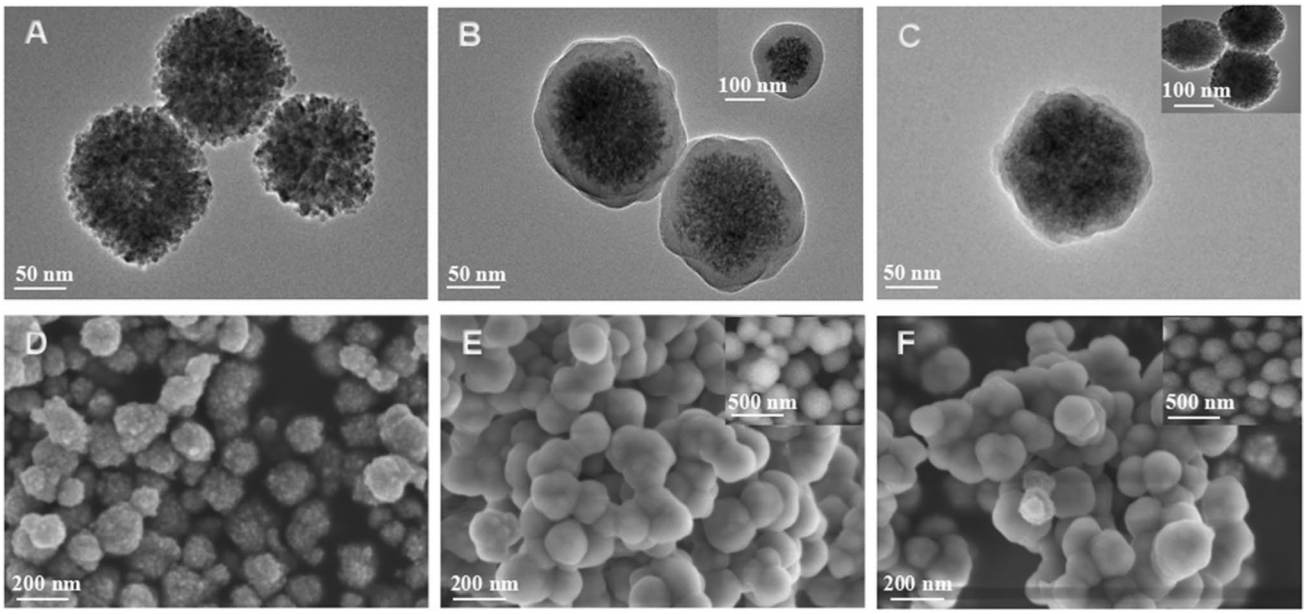

Fig. 2 TEM images of Fe_3O_4 (**A**), Fe_3O_4@SiO_2 (**B**), Fe_3O_4@C (**C**). SEM images of Fe_3O_4 (**D**), PTL-coated Fe_3O_4@SiO_2 (**E**), PTL-coated Fe_3O_4@C (**F**). The inset shows TEM images of PTL-coated Fe_3O_4@SiO_2 (**B**) and PTL-coated Fe_3O_4@C (**C**); SEM images of Fe_3O_4@SiO_2 (**E**) and Fe_3O_4@C (**F**)

Supplementary Material). The PTL-coated MNPs possessed similar diffraction pattern with Fe_3O_4 nanocrystal in XRD patterns (Fig. 3C), demonstrating that the crystal phase of Fe_3O_4 was unchanged after modification. Furthermore, the maximum saturation magnetization (M_S) of Fe_3O_4@C and Fe_3O_4@SiO_2 MNPs were less than the corresponding bulk Fe_3O_4 due to the existence of nonmagnetic carbon/silicon shells. The M_S value of Fe_3O_4@SiO_2 MNPs was lower than that of Fe_3O_4@C MNPs (Fig. 3D), which demonstrated the higher thickness of the SiO_2 shells

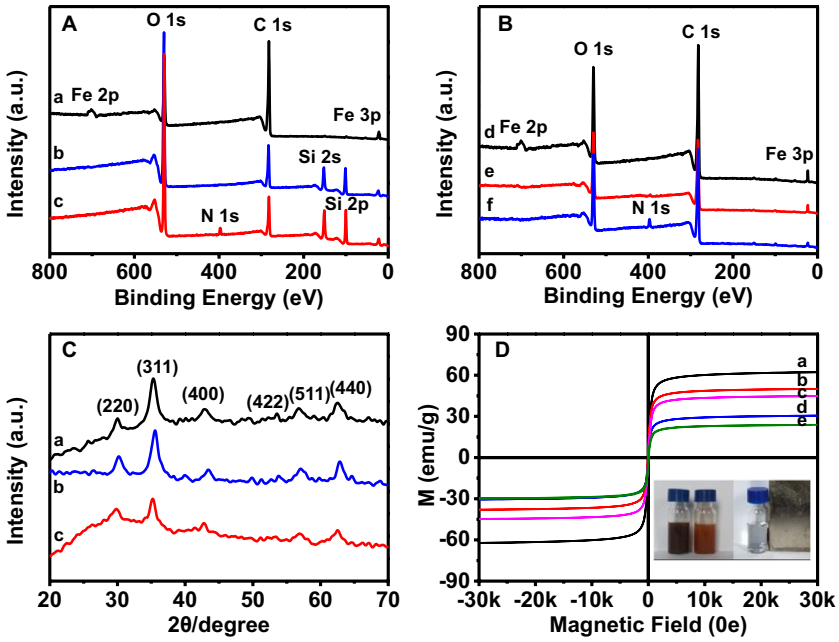

Fig. 3 XPS spectra of (**A** and **B**): Fe_3O_4 (a, d), Fe_3O_4@SiO_2 (b), PTL-coated Fe_3O_4@SiO_2 MNPs (c), Fe_3O_4@C (e), and PTL-coated Fe_3O_4@C (f). XRD spectra of C: Fe_3O_4 (a), PTL-coated Fe_3O_4@SiO_2 (b), and PTL-coated Fe_3O_4@C MNPs (c). Magnetic hysteresis curves of (**D**): Fe_3O_4 (a), Fe_3O_4@C (b), PTL-coated Fe_3O_4@C (c), Fe_3O_4@SiO_2 (d), and PTL-coated Fe_3O_4@SiO_2 MNPs (e). Photographs of PTL-coated Fe_3O_4@C and Fe_3O_4@SiO_2 MNPs solutions before and after magnetic separation

than the C shells and also correlated to the TEM observation results (Fig. 2B, C). Furthermore, the M_S values with no changes in the PTL-coated MNPs were observed. The materials can achieve rapid magnetic separation within a few seconds from solution, indicating good water solubility and dispersibility (Fig. 3D, inset).

Finally, the surface properties of the synthesized MNPs were characterized by ATR-FTIR. A characteristic absorption peak at ~ 580 cm^{-1} was assigned to stretching vibration of Fe–O in Fe_3O_4 MNPs (Fig. 4A, C). Meanwhile, a new peak at 1100 cm^{-1} was attributed to the symmetric stretching vibration of the Si–O–Si bond in Fe_3O_4@SiO_2 MNPs (Fig. 4Ab), and the peaks at 1620 and 1701 cm^{-1} corresponded to C = C and C = O vibrations on the Fe_3O_4@C MNPs (Fig. 4Cd), respectively, indicating that the silica and carbon shells were successfully constructed around Fe_3O_4 MNPs. After assembled with PTL nanofilms, the peaks at 1621 cm^{-1} and 1635 cm^{-1} were associated with the amide I

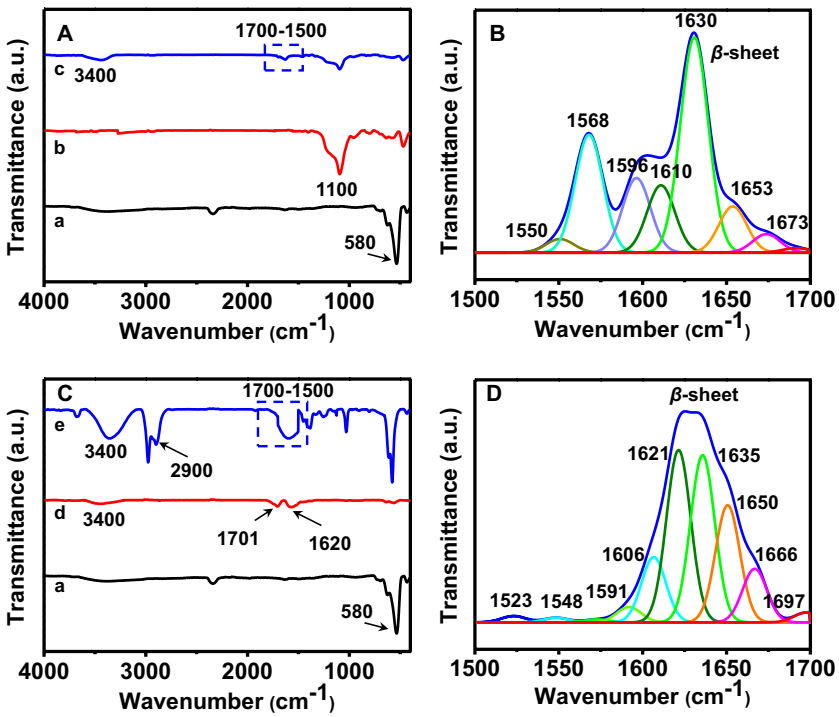

Fig. 4 ATR-FTIR spectra of (**A** and **C**): Fe_3O_4 (a), Fe_3O_4@SiO_2 (b), PTL-coated Fe_3O_4@SiO_2 (c), Fe_3O_4@C (d) and PTL-coated Fe_3O_4@C (e); The corresponding deconvolution of the amide I and II regions for PTL-coated Fe_3O_4@SiO_2 and Fe_3O_4@C (**B** and **D**), respectively

band and N–H bond mainly corresponding to β-sheet structure, showing the successful loading of PTL nanofilms on the Fe_3O_4@SiO_2 and Fe_3O_4@C MNPs (Fig. 4B, D).

Specific phosphopeptide enrichment from the tryptic standard protein and human serum digests by Ti^{4+}-PTL-MNPs

We explored the applicability of the fabricated Ti^{4+}-PTL-MNPs for selective enrichment of phosphopeptides (β-casein digests). As can be seen, three typical phosphopeptide peaks (m/z ≈ 2,061, 2,566, and 3,122) were identified with high intensities after enrichment by the fabricated Ti^{4+}-PTL-MNPs (Fig. 5A, B). By contrast, almost no phosphopeptide peaks were observed in protein digests whether directly analyzed (Fig. 5, insets) or enriched by Ti^{4+}-Fe_3O_4@SiO_2 (Fig. 5C) and Ti^{4+}-Fe_3O_4@C (Fig. 5D) in protein digests. The sequences of three typical phosphopeptide peaks were presented in Table S1 (see Electronic Supplementary Material). The above results clearly demonstrated the excellent stability and high specificity of the fabricated Ti^{4+}-PTL-MNPs for phosphopeptide enrichment. Moreover, adsorption time and the loading buffer with different HAC concentrations were optimized, and the optimized experimental parameters were 2% HAC + 50% ACN buffer with the best adsorption time of 3 min (Fig. S2, see Electronic Supplementary Material).

The selectivity in phosphopeptides enrichment by Ti^{4+}-PTL-MNPs was researched under the existence of nonphosphorpeptides. The mixtures of phosphopeptides and nonphosphopeptides with mass ratio of 1:200 and 1:400 was used as the models. Before enrichment, no phosphopeptide peaks were detected in the MS analysis (Fig. 6, inserts), presumably due to severe signal interference and suppression of massive nonphosphopeptides. In contrast, three typical phosphopeptide peaks were detected at the ratio of 1:200 with high intensities and low interference after enrichment with the Ti^{4+}-PTL-MNPs (Fig. 6A, B). Even if the mass ratio was as low as 1:400, three typical phosphopeptide peaks were also captured successfully (Fig. 6C, D). The quantitative recovery of phosphopeptides was also calculated after treated with Ti^{4+}-PTL-MNPs. As shown in Table S2 (see Electronic Supplementary Material), the recovery of standard phosphopeptides were at least 88% and 89% for Ti^{4+}-PTL-Fe_3O_4@SiO_2 and Ti^{4+}-PTL-Fe_3O_4@C, respectively. These results manifested the highly specific enrichment of phosphopeptides of the Ti^{4+}-PTLMNPs in the presence of high concentrations of interfering nonphosphopeptides, which was well comparable to previously reported materials [35, 38].

The sensitivity of the Ti^{4+}-PTL-MNPs for phosphopeptide capturing was explored using tryptic digests of β-casein with different concentrations (1, 0.1, and 0.01 fmol μL^{-1}). As shown in Fig. S3 (see Electronic Supplementary Material), even at a low concentration (0.01 fmol μL^{-1}), three typical phosphopeptide peaks can be detected, indicating the high sensitivity of the fabricated Ti^{4+}-PTL-MNPs. The Ti^{4+}-PTL-MNPs were thoroughly washed and reused for enrichment of β-casein digests (0.1 fmol μL^{-1}). Furthermore, the recyclability and regeneration of the Ti^{4+}-PTL-MNPs was also conducted through repeatedly washing materials with the buffer and water. As shown in Fig. S4 (see Electronic Supplementary Material), three typical phosphopeptide peaks in β-casein digests were still clearly detected with slight decrease of intensities even after six cycles, indicating the good reusability of the Ti^{4+}-PTL-MNPs towards phosphopeptides. Compared with other metal ions-immobilized materials (Table S3, see Electronic Supplementary Material), the Ti^{4+}-PTL-MNPs

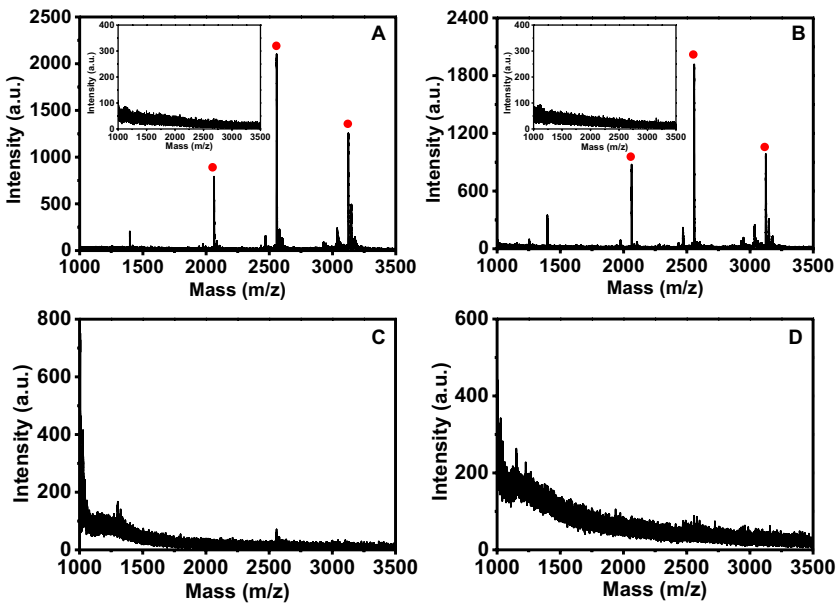

Fig. 5 MALDI-TOF mass spectra of the tryptic standard β-casein digests. Analyses after the enrichment with Ti^{4+}-PTL-Fe_3O_4@SiO_2 (A), Ti^{4+}-PTL-Fe_3O_4@C (B), Ti^{4+}-Fe_3O_4@SiO_2 (C), and Ti^{4+}-Fe_3O_4@C (D). The insets are the MALDI-TOF MS of the β-casein digests without enrichment. Phosphopeptides are marked with a solid red circle

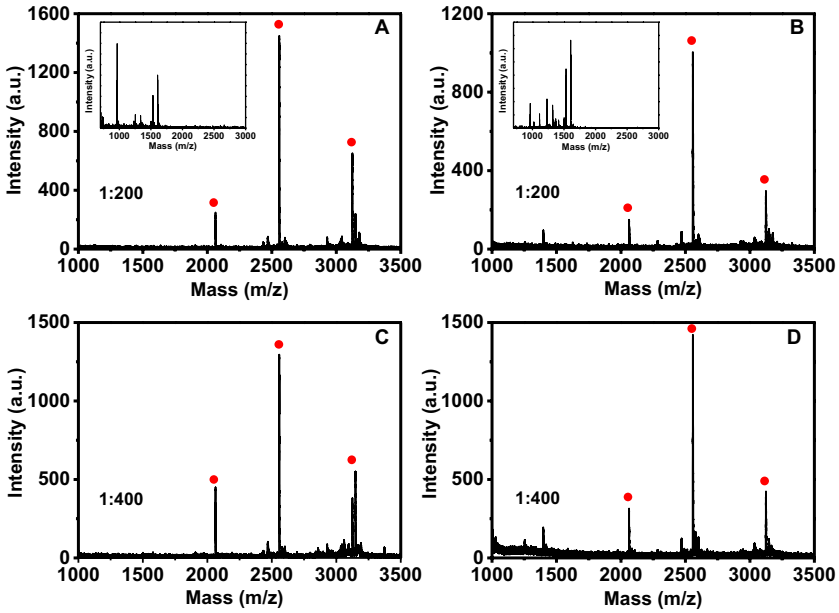

Fig. 6 Enrichment of phosphopeptides with the Ti^{4+}-PTL-MNPs from different mass ratios of β-casein and BSA digests. Insets in (**A**) and (**B**) are direct analyses for the mass ratio of 1:200. Enrichment at mass ratios of 1:200 (**A**, **B**) and 1:400 (**C**, **D**) with Ti^{4+}-PTL-Fe_3O_4@SiO_2 and Ti^{4+}-PTL-Fe_3O_4@C, respectively. Phosphopeptides are marked with a solid red circle

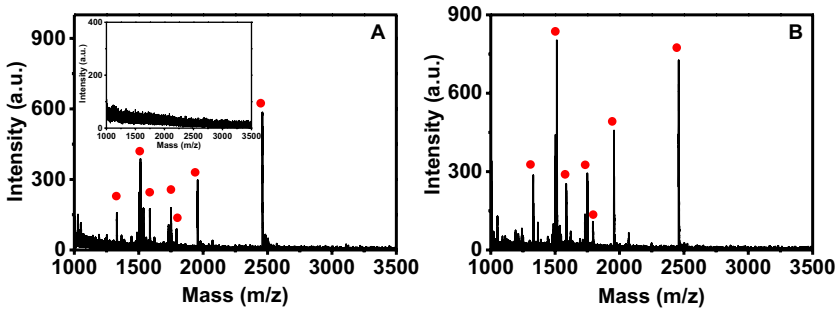

Fig. 7 MALDI-TOF MS analysis of the human serum captured (inset) without treatment and the enrichment using Ti^{4+}-PTL-Fe_3O_4@SiO_2 (**A**) and Ti^{4+}-PTL-Fe_3O_4@C (**B**). Phosphopeptides are marked with a solid red circle

exhibited the high sensitivity and selectivity for capturing phosphopeptides from intricate samples.

In clinical medicine, endogenous serum phosphopeptides may be used as biomarkers in many physiological diseases analysis. Whereas the complexity and codependent proteins in human serum, highly specific enrichment of phosphopeptides was always a great challenge. Encouraged by its excellent sensitivity and selectivity, the fabricated Ti^{4+}-PTL-MNPs were further applied for the enrichment of phosphopeptides in human serum. As Fig. 7 showed, no phosphopeptide peaks were detected without treatment for the inhibition and interference of the complex sample. After treated with Ti^{4+}-PTL-Fe_3O_4@SiO_2 (Fig. 7A) and Ti^{4+}-PTL-Fe_3O_4@C (Fig. 7B), seven phosphopeptide signals were observed with high intensity. The phosphopeptide sequences were provided in Table S4 (see Electronic Supplementary Material). The Ti^{4+}-PTL-MNPs showed high capability in specific trapping phosphopeptides in complex biological samples compared with other reported affinity materials (Table S3, see Electronic Supplementary Material).

Conclusions

In summary, we proposed a simple and green approach via a one-step aqueous self-assembly PTL nanofilms for Ti^{4+}-PTL-MNPs fabrication, which were used as effective adsorbents for enriching trace amounts of phosphopeptides from standard proteins (β-casein) and human serum. The PTL nanofilms with abundant chelating sites for efficiently binding Ti^{4+} remained intact after repeated washing with an acidic organic solution and ultrasonication, showing their remarkable mechanical stability. Measured by MALDI-TOF MS, the fabricated Ti^{4+}-PTL-MNPs had a sensitivity of 0.01 fmol μL^{-1} and high selectivity of 1:400 (mass ratios of β-casein to BSA digests). Moreover, good stability and reusability of the fabricated Ti^{4+}-PTL-MNPs were confirmed by their high enrichment performance with β-casein digests for six cycles. This study provides a convenient and ecofriendly method for surface functionalization of adsorbents for selective enrichment of phosphopeptides in phosphoproteomics study.

Supplementary information The online version contains supplementary material available at https://doi.org/10.1007/s00216-024-05170-7.

Acknowledgements This work was supported by the Natural Science Foundation Project of Shaanxi Province (No. 2020JZ-24), the National Key R&D Program of China (2019YFB2103000), and the Fundamental Research Funds for the Central Universities (GK201801006).

Author contributions Jianru Li & Nan Li: Conceptualization, Methodology, Investigation, Validation, Writing—original draft, Writing—review & editing. Yawen Hou: Investigation, Validation. Miao Fan & Yuxiu Zhang & Qiqi Zhang: Resources. Fuquan Dang: Supervision, Funding acquisition.

Funding National Key R&D Program of China, 2019 YFB2103000, Fundamental Research Funds for the Central Universities, GK201801006, Natural Science Foundation Project of Shaanxi Province, No. 2020JZ-24

Declarations

Conflict of interest The authors declare that they have no known competing financial interests or personal relationships that could have appeared to influence the work reported in this paper.

Ethics statement Human serum was obtained from Shaanxi Normal University Hospital. All the experiments were permitted by Human Research Ethics Board of Shaanxi Normal University (NO. 20150323). All participants provided written informed consent.

References

1. Li XS, Yuan BF, Feng YQ. Recent advances in phosphopeptides enrichment: strategies and techniques. TrAC-Trends Anal Chem. 2016;78:70–83.
2. Li YN, Wang Y, Dong MM, Zou HF, Ye ML. Sensitive approaches for the assay of the global protein tyrosine phosphorylation in complex samples using a mutated SH_2 domain. Anal Chem. 2017;89:2304–11.
3. Lyu JW, Wang Y, Mao JW, Yao YT, Wang SJ, Zheng Y, Ye ML. A pseudo-targeted MS method for the sensitive analysis of protein phosphorylation in protein complexes. Anal Chem. 2018;90:6214–21.
4. Li M, Xiong Y, Qing G. Innovative chemical tools to address analytical challenges of protein phosphorylation and glycosylation. Acc Chem Res. 2023;56(18):2514–25.
5. Demon B, Aebersold R. Mass spectrometry and protein analysis. Science. 2006. https://doi.org/10.1126/science1124619.
6. Kennedy RT. The 2019 Reviews Issue. Anal Chem. 2019;91:1–1.
7. Han DQ, Yao ZP. Chiral mass spectrometry: An overview. TrAC-Trends Anal Chem. 2020;123: 115763.
8. Gao RF, Li J, Shi R, Zhang Y, Ouyang FZ, Zhang T, Hu LH, Xu GQ, Lian J. Highly sensitive detection of phosphopeptides with superparamagnetic Fe_3O_4 @$mZrO_2$ core-shell microspheres-assisted mass spectrometry. J Mater Sci Technol. 2020;59:234–42.
9. Ng CC, Zhou Y, Yao ZP. Algorithms for de-novo sequencing of peptides by tandem mass spectrometry: A review. Anal Chim Acta. 2023;1268.
10. Cheng G, Zhang JL, Liu YL, Sun DH, Ni JZ. Synthesis of novel Fe_3O_4@SiO_2@CeO_2 microspheres with mesoporous shell for phosphopeptide capturing and labeling. Chem Commun. 2011;47:5732–4.
11. Lin H, Yuan K, Deng C. Preparation of a TiO_2-NH_2 modified MALDI plate for on-plate simultaneous enrichment of phosphopeptides and glycopeptides. Talanta. 2017;175:427–34.
12. Guo HH, Chen G, Ma JT, Jia Q. A triazine based organic framework with micropores and mesopores for use in headspace solid phase microextraction of phthalate esters. Microchim Acta. 2019;186:DOI: 101007/s00604–018–3060–7.
13. Zhang Y, Wang B, Jin W, Wen Y, Nan L, Yang M, Liu R, Zhu Y, Wang C, Huang L, Song X, Wang Z. Sensitive and robust MALDI-TOF-MS glycomics analysis enabled by Girard's reagent T on-target derivatization (GTOD) of reducing glycans. Anal Chim Acta. 2019;1048:105–14.
14. Gao L, Uttamchandani M, Yao SQ. Comparative proteomic profiling of mammalian cell lysates using phosphopeptide microarrays. Chem Commun. 2012;48:2240–2.
15. Nilsson CL. Advances in quantitative phosphoproteomics. Anal Chem. 2012;84:735–46.
16. Alcolea MP, Cutillas PR. In-depth analysis of protein phosphorylation by multidimensional ion exchange chromatography and mass spectrometry. Methods in Mol Biol. 2010;658:111–26.
17. Yang S, Chang Y, Zhang H, Yu X, Shang W, Chen G, Chen DY, Gu Z. Enrichment of phosphorylated peptides with metal-organic framework nanosheets for serum profiling of diabetes and phosphoproteomics analysis. Anal Chem. 2018;90:13796–805.
18. Gao L, Tao J, Qi L, Jiang X, Shi H, Liu Y, Di B, Wang Y, Yan F. Synthesis of a metal oxide affinity chromatography magnetic mesoporous nanomaterial and development of a one-step selective phosphopeptide enrichment strategy for analysis of phosphorylated proteins. Anal Chim Acta. 2022;1195.
19. Wang Y, Li P, Xu W, Zhang D, Jia Q. Hydrophilic magnetic host-guest Ti-phenolic networks: a promising material for the highly sensitive enrichment of glycopeptides and phosphopeptides. J Mater Chem B. 2023;11(22):4874–81.
20. Zhao Y, Xu W, Zheng H, Jia Q. Light, pH, and temperature triple-responsive magnetic composites for highly efficient phosphopeptide enrichment. Anal Chem. 2023;95(23):9043–51.
21. Wang Z, Wang J, Sun N, Deng C. A promising nanoprobe based on hydrophilic interaction liquid chromatography and immobilized metal affinity chromatography for capture of glycopeptides and phosphopeptides. Anal Chim Acta. 2019;1067:1–10.
22. Xu Z, Wu Y, Wu H, Sun N, Deng C. Hydrophilic polydopamine-derived mesoporous channels for loading Ti (IV) ions for salivary phosphoproteome research. Anal Chim Acta. 2021;1146:53–60.
23. Li N, Zhang L, Shi HL, Li JR, Zhang J, Zhang ZQ, Dang FQ. Specific enrichment of phosphopeptides by using magnetic nanocomposites of type Fe_3O_4@graphene oxide and Fe_3O_4@C coated with self-assembled oligopeptides. Microchim Acta. 2020;187:144.
24. Veleva VR, Cue BW, Todorova Jr. Benchmarking green chemistry adoption by the global pharmaceutical supply chain. ACS Sustainable Chem Eng. 2018;6:2−14.
25. Wang H, Tian ZX. Facile synthesis of titanium (IV) ion immobilized adenosine triphosphate functionalized silica nanoparticles for highly specific enrichment and analysis of intact phosphoproteins. J Chromatogr A. 2018;1564:69–75.
26. Jiang DD, Li XQ, Ma JT, Jia Q. Development of Gd^{3+}-immobilized glutathione-coated magnetic nanoparticles for highly selective enrichment of phosphopeptides. Talanta. 2018;180:368–75.
27. Luo B, Zhou XX, Jiang PP, Yi QY, Lan F. PAMA-Arg brush-functionalized magnetic composite nanospheres for highly effective enrichment of phosphorylated biomolecules. J Mater Chem B. 2018;6:3969–78.
28. Liu R, Zhao J, Han Q, Hu X, Wang D, Zhang X, Yang P. One-step assembly of a biomimetic biopolymer coating for particle surface engineering. Adv Mater. 2018;30:1802851.

29. Wang K, Li N, Hai XM, Dang FQ. Lysozyme-mediated fabrication of well-defifined core-shell nanoparticle@metal-organic framework nanocomposites. J Mater Chem A. 2017;5:20765–70.
30. Pan MR, Sun YF, Zheng J, Yang WL. Boronic acid-functionalized core-shell-shell magnetic composite microspheres for the selective enrichment of glycoprotein. ACS Appl Mater Interfaces. 2013;5:8351–8.
31. Zhang QQ, Hang YY, Jiang BY, Hu YJ, Xie JJ, Gao X, Jia B, Shen HL, Zhang WJ, Yang PY. In situ synthesis of magnetic mesoporous phenolic resin for the selective enrichment of glycopeptides. Anal Chem. 2018;90:7357–63.
32. Liu J, Sun ZK, Deng YH, Zou Y, Li CY, Guo XH, Xiong LQ, Gao Y, Li FY, Zhao DY. Highly water-dispersible biocompatible magnetite particles with low cytotoxicity stabilized by citrate groups. Angew Chem Int Ed. 2009;48:5875–9.
33. Chen ZM, Geng ZR, Zhang ZY, Ren LB, Tao TX, Yang RC, Guo ZX. Synthesis of magnetic Fe_3O_4@C nanoparticles modified with -SO_3H and -COOH groups for fast removal of Pb^{2+} Hg^{2+} and Cd^{2+} ions. Eur J Inorg Chem. 2014;3172−3177.
34. Yan YH, Zheng ZF, Deng CH, Zhang XM, Yang PY. Facile synthesis of Ti^{4+}-immobilized Fe_3O_4@polydopamine core-shell microspheres for highly selective enrichment of phosphopeptides. Chem Commun. 2013;49:5055–7.
35. Qi DW, Mao Y, Lu J, Deng CH, Zhang XM. Phosphate-functionalized magnetic microspheres for immobilization of Zr^{4+} ions for selective enrichment of the phosphopeptides. J Chromatogr A. 2010;1217:2606–17.
36. Gu J, Su Y, Liu P, Li P, Yang P. An environmentally benign antimicrobial coating based on a protein supramolecular assembly. ACS Appl Mater Interfaces. 2016;9:198–210.
37. Gu J, Miao S, Yan Z, Yang P. Multiplex binding of amyloid-like protein nanofilm to different material surfaces. Colloid Interface Sci Commun. 2018;22:42–8.
38. Wang HP, Jiao FL, Gao FY, Lv YY, Wu Q, Zhao Y, Shen YH, Zhang YJ, Qian XH. Titanium (IV) ion-modified covalent organic frameworks for specific enrichment of phosphopeptides. Talanta. 2017;166:133–40.